Short Communication

Electrochemical Investigation of Testosterone Using a AuNPs Modified Electrode

Zhuangzhuang Sun[1], Yuan An[1], Hui Li[1], Hui Zhu[2,] and Meisong Lu[1, *]*

[1] Department of Reproductive Medicine, The first Affiliated Hospital of Harbin Medical University, Harbin, Heilongjiang, 150001, P.R. China
[2] Department of Physiology, The college of Basic Medical Sciences, Harbin Medical University, Harbin, Heilongjiang, 150086, P.R. China
[*]E-mail: huizhu0872@sina.com, Meisonglu0417@163.com

Polycystic ovarian syndrome (PCOS) is a disease that occurs extensively among females during their reproductive period and that can be diagnosed using the testosterone level in the body. In the present report, a biosynthesized gold nanoparticle (AuNP)-based electrochemical impedance immunosensor was fabricated for the first time and used for the detection of testosterone with a wide detection range of 10 ng/mL - 0.5 μg/mL. In addition, our proposed immunosensor showed excellent performance in the detection of testosterone in saliva specimens.

Keywords: Polycystic ovarian syndrome; Electrochemical impedance immunosensor; Testosterone; Saliva; Biosynthesis

1. INTRODUCTION

Polycystic ovarian syndrome (PCOS) is a disease that occurs extensively among females during their reproductive period. One standard PCOS diagnostic tool is the determination of the testosterone hormone level, which usually increases in the case of PCOS [1-5]. In the ovaries of females, theca interna is transformed into estradiol, contributing to the synthesis of testosterone in small quantities [6-8]. Testosterone generated in females is carried via blood, where the sex-hormone binding globulin (SHBG)-bound form, albumin-bound form, and the free form account for 66–78%, 20–30%, and 2%, respectively, of the total testosterone content [9-11]. Normally, bioavailable testosterone refers to the sum of the latter two forms as the only testosterone available for tissue exchange, whereas the first form is biological inactive. Based on the literature, no traditional

measurement techniques (e.g., RIA [12, 13]) have been found to be sufficiently sensitive for the direct quantification of free testosterone in a protein-free ultrafiltrate of plasma. On the other hand, serum-free testosterone can be determined using equilibrium dialysis (reference method), whereas this technique is unavailable in most clinical labs considering the sophistication of the testing system [14-16].

The measurement of free testosterone in serum using extensively applied radioimmunoassay (RIAs) has been shown to be inaccurate, motivating the development of other, more accurate assessment strategies [17-20]. In the field of diagnostics, saliva has also been used as a study tool for disease processes and disorders. Significant data for the functioning mechanism of different organs within the body has been provided by analyzing saliva samples. The identification of testosterone in saliva has been achieved, and investigations of the reliability of salivary testosterone analysis are expected in order to determine the good correlation with the concentration of serum testosterone [21-23]. Testosterone is secreted in saliva, and the free form, but not the albumin-bound and SHBG [24-26] forms, can be detected.

To detect and quantify the testosterone content in biological fluids, chromatographic techniques have been reported, including HPLC [27, 28], GC–MS [29, 30] and LC–MS [31, 32], which are highly selective and sensitive in quantitative detection. However, these methods are highly time-consuming and usually require the use of certain costly devices. Thus, the normal application of these methods under laboratory conditions is restricted due to these limitations [33-37]. For the analytes involved in biologically vital reactions of oxidation and/or reduction, such as pharmaceutical dosage forms of isolated drugs and related molecules, electrochemical methods using modified electrodes show distinct versatility and sensitivity [38-40], as they are relatively specific, sensitive, low cost, extremely simple, and require comparatively short analysis time.

The present work presents testosterone detection using a sensitive and novel electrochemical immunosensor based on the combination of biosynthesized-AuNP-modified electrodes, where the antitestosterone was directly attached onto the surface of the electrode. The distinct features of the AuNPs in terms of the immobilization of biomolecules retaining their biological activity and serving as effective conductive interfaces led to an enhancement in the electrode kinetics. In addition, our developed electrochemical immunosensor exhibited excellent detection of testosterone in saliva samples.

2. EXPERIMENTS

2.1. Chemicals

Phosphate buffered saline (PBS) that contained Na_2HPO_4 (0.1 mM), KCl (2.7 mM), NaCl (140 mM), and KH_2PO_4 (1.8 mM), pH 7.2, was used throughout the measurements, with a redox mediator (10 mM $K_3[Fe(CN)_6]/K_4[Fe(CN)_6]$) added if appropriate. 2-Mercaptoethylamine (2-MEA) hydrochloride, 3-mercaptopropionic acid (MPA), monoclonal murine antitestosterone (Ag-estosterone), and $HAuCl_4$ were commercially available from Sigma-Aldrich Corp. Testosterone (Ab-

estosterone) was commercially available from Biospecific and was diluted using the as-prepared PBS to obtain a 10 µg/mL solution. Mill-Q water was used for washing. Fresh *Pithophora oedogonia* was collected from Harbin Jinhewan Wetland Botanical Garden. *Pithophora oedogonia* was washed to yield a wet sample. After drying in the dark for 3 d, this sample was left to thoroughly dry in an oven at 70°C. This as-prepared sample was ground into a fine powder prior to further use. Other reagents were of analytical grade and used without further purification.

2.2. AuNPs synthesis

AuNPs were synthesized by first adding *Pithophora oedogonia* powder (10 g) to water (100 mL), followed by sonication for 15 min, and then heat treating at 70 °C for an additional 15 min. Filter paper (pore size: 200 nm) was used for the filtration of this as-prepared extract. For the synthesis of Au nanoparticles, the as-prepared sample extract (20 mL) was added to a $HAuCl_4$ solution (20 mL) under sonication for 60 min. Then, Au nanoparticles were formed, as evidenced by the color change from light yellow into purplish yellow. Afterwards, the final Au nanoparticles were obtained after separation using centrifugation for 0.5 h at 10,000 rpm and washing. Finally, the nanoparticles were left to dry in an oven at 70°C. AuNPs were functionalized by the following processes. First, the AuNP solution was stabilized by immediately adding a mixture of H_2O (10 mL) and MPA (46 µL) to obtain a final volume of 50 mL. The mixed solution was stirred at ambient temperature for 120 min. This was followed by washing the obtained colloidal solution using ethanol for two to three times, centrifugation at 20000 rpm, and drying under vacuum for 12 h.

2.3. Immunosensor fabrication

Initially, ITO-coated glass plates were ultrasonically cleaned sequentially and dried under vacuum. The amount of hydroxyl groups on the surface of ITO glass was increased by exposing the as-prepared ITO glass plates to oxygen plasma in a plasma chamber for 5 min. Afterwards, a SAM of APTES was formed by immersing the plates into an APTES solution (2%) synthesized in ethanol in ambient atmosphere for 90 min. The unbonded APTES was removed from the substrate surface after ethanol rinsing. Then, the samples were left to dry under N_2 gas flow to obtain APTES/ITO glass plates. After immersion in the as-prepared mixture of functionalized Au(MPA) nanoparticles for 3 h, the plates were washed using doubly distilled water and dried under N_2 gas flow. Then, the final product was obtained as Au(MPA-NHS)/APTES/ITO glass. For the immobilization of Ab-testosterone onto this electrode, it was treated with PBS that contained Ab-testosterone (10 µg/mL) overnight at 4 °C, washed using PBS, and dried under N_2 flow to obtain the Ab-testosterone-immobilized electrode (denoted as Ab-testosterone/Au(MPA)/APTES/ITO glass). For this electrode, the nonspecific binding sites present on its surface were blocked after incubation in 1% BSA solution for 0.5 h, and all physically adsorbed antibodies were removed after washing using PBS. Finally, the Ab-testosterone-immobilized electrode was left to dry under N_2 flow.

2.4. Electrochemical determination

Testosterone was electrochemically determined with a three-electrode configuration, where the reference and counter electrodes were saturated Ag/AgCl and a Pt foil, respectively. Electrochemical impedance spectroscopy (EIS) was carried out in pH 7.4 PBS (0.1 M KCl) solution that contained 2 mM $[Fe(CN)_6]^{3-}/[Fe(CN)_6]^{4-}$ under the following parameters: AC voltage, 0.05 V; frequency, 1 Hz - 100 kHz. In PBS, aliquots from 100 µg/mL Ag-testosterone (stock solution) at varying concentrations were prepared. Aliquots of Ag-testosterone at varying concentrations were added successively into the PBS solution that contained 2 mM $[Fe(CN)_6]^{3-}/[Fe(CN)_6]^{4-}$ to obtain the EIS results of the Ab-testosterone /Au(MPA)/APTES/ITO glass bioelectrode. An impedance measurement was carried out using a sample solution in the absence of Ag-testosterone, and the control sample response for the corresponding electron-transfer resistance (R_{et}) was recorded in a Nyquist plot. The immunoreactions between antigen and antibody were determined by measuring the R_{et} values and other EIS parameters by successively adding aliquots of Ab-testosterone at varying concentrations.

3. RESULTS AND DISCUSSION

For the test, the biosynthesis reaction was initiated upon the addition of *Pithophora oedogonia* extract to the $HAuCl_3$ solution, with the initial nucleation of Au nanoparticles suggested by the slow color transformation of the dispersed solution from light yellow to purplish yellow. Light at a certain wavelength could be absorbed by the scattered metallic nanoparticles. Thus, the surface plasmon resonances of the AuNPs can be monitored in the as-prepared AuNP dispersion. We note that several characteristics such as size, solvent and morphology will influence the optical properties of the AuNPs [41]. Due to the light scattering and absorption of the metallic nanoparticles at a particular wavelength, the obtained Au nanoparticle dispersion exhibited surface plasmon resonances of the AuNPs. The UV-vis spectrum (UVs) of the AuNPs prepared in the presence of *Pithophora oedogonia* is shown in Fig. 1 A. The spectrum showed an obvious absorption peak at 525 nm, corresponding to the surface plasmon resonance of the AuNPs and confirming that the metallic Au material was formed. The mean size of the obtained AuNPs is reflected by the location of the surface plasmon resonance peak. XPS results also provided convincing evidence that the AuNPs were formed.
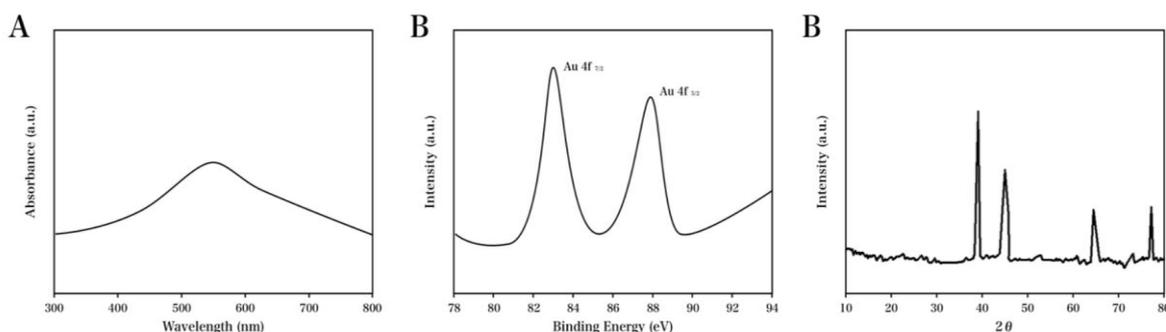

Figure 1. (A) UV-vis spectrum, (B) High resolution Au 4f scan and (C) XRD pattern of biosynthesized Au nanoparticles.

The capability to measure the properties of monolayer films is a remarkable advantage of cyclic voltammetry. These films would impede the shift reactions at the interface of the electrolyte and the electrode modified by APTES. We note that in this blocking mechanism, a redox couple was employed as a probe molecule. The peak-to-peak potential separation (ΔEp) was approximately 50 mV, and the ratio of the redox peak current Ipa/Ipc was approximately 1, suggesting that the electrochemical reaction is reversible as a result of the construction of the AuNPs. The small peak-to-peak separation indicated a fast electron-transfer rate [42, 43]. The as-prepared AuNPs were also characterized via a Au_{4f} high-resolution XPS scan, as shown in Fig. 1B. The $Au_{4f\,5/2}$ peak was observed at 87.2 eV, and the $Au_{4f\,7/2}$ peak was observed at 83.5 eV. Considering the surface attachment of biomolecules from the *Pithophora oedogonia* extract, the peaks exhibited a theoretical value shift of Au^0 at 84.0 and 87.7 eV. The as-prepared AuNPs were further characterized via their XRD profile, as shown in Fig. 1C. Diffraction peaks were observed at 39.3°, 45.9°, 67.7° and 81.9°, corresponding to the (111), (200), (220) and (311) planes of the face-centered-cubic (fcc) crystallographic structure of Au (JCPDS 4-0783), respectively. The above results suggested that metallic Au was successfully formed.

APTES/ITO, Au(MPA)/APTES/ITO and Au-testosterone/Au(MPA)/APTES/ITO were characterized via FTIR patterns (attenuated total reflection mode), as shown in Fig. 2. The Si–O–Si characteristic band was observed at 1051 cm^{-1} for APTES. The characteristic peak at 1747 cm^{-1} corresponded to the C=O stretching vibrations of the carboxylic groups present in the MPA-functionalized AuNPs. The peaks observed at 934 cm^{-1} corresponded to the –OH bending vibrations of the carboxylic acid groups, and the peaks observed at 2961 cm^{-1} were due to the –OH stretching vibrations of the carboxylic acid group. Further peaks were observed at 1613 and 3385 cm^{-1} after Ab-testosterone was immobilized, corresponding to the N–H bending and stretching vibrations, respectively. The above results indicated that amide bonds were formed between the Ab-testosterone molecules and Au(MPA) nanoparticles.
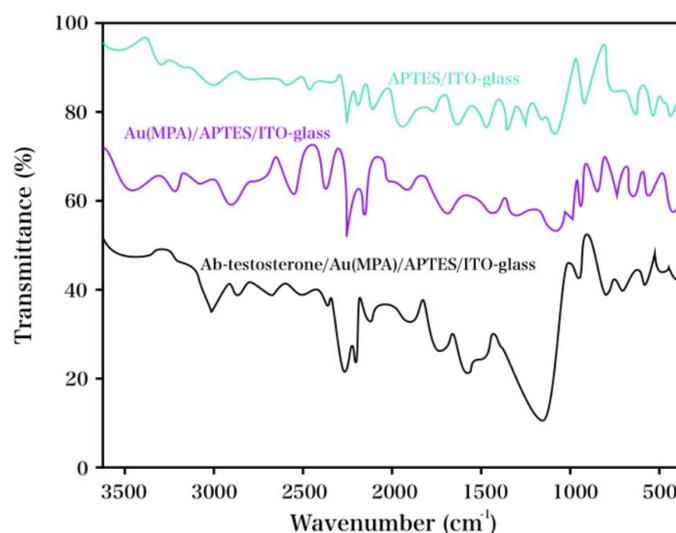

Figure 2. FTIR spectra of APTES/ITO-glass, Au(MPA)/APTES/ITO-glass and Ab-testosterone/Au(MPA)/APTES/ITO-glass.

As a useful technique for qualitative and quantitative characterization of electrochemical reactions at the interface of the solution and electrode, EIS is considered a dominant measurement for the assessment of immunosensor behavior. It is known that changes in electrochemical impedance reflect chemical processes occurring on electrochemical sensors [44]. The response of the proposed configuration to varying frequencies and a small AC signal amplitude was monitored by EIS. Important parameters for the rates of the reactions at the interface of solution and electrode were recorded, even though the chemical bonds or intermediates could not be identified using this method. Here, an 'equivalent circuit' consisting of an assembly of electrical circuit elements was used for the modeling of the physicoelectric properties of this interface. The experimentally fit Randles equivalent circuit model used in this report included four parameters, including R_s (ohmic resistance of the electrolyte solution), Z_w (Warburg impedance, referring to the ion diffusion from the bulk electrolyte to the electrode interface), C_{dl} (interfacial double layer capacitance between the solution and electrode, associated with the electrode surface condition), and R_{et} (electron-transfer resistance). For the modification of the above equivalent circuit model, the classical capacitance was replaced with a constant phase element (CPE) to incorporate the electrode surface heterogeneity or roughness with the Helmholtz double layer. Additionally, CPE was arranged in parallel with Z_w and R_{et}, and all these were arranged in series with R_s. The equation below represented the CPE-related impedance:

$$Z_{CPE}(\omega) = 1 / Y_0 (j\omega)^n$$

where Y_0 is a constant, j is an imaginary number, ω is the angular frequency, and n is the CPE exponent, used as a gauge of the heterogeneity and offering detailed information on the surface inhomogeneity degree. Based on n, the CPE could correspond to resistance, capacitance ($n = 1$, $Y_0 = C$), inductance ($n = -1$) or Warburg element ($n = 0.5$). The exponent n is *ca.* 1, indicating minimal defects in the modification layer on the surface of the electrode. This result further suggested the resemblance of the CPE to a pseudocapacitor in the present case. The impedance performances of differently modified electrodes were indicated through the Nyquist plots (the real part of the impedance Z' *vs.* the imaginary part $-Z''$). Typically, the plots have two dominant regions: (i) a semicircle at high frequencies, corresponding to the Faradaic electron-transfer process (R_{et}: the diameter of the semicircle); and (ii) a linear region at lower frequencies, suggesting the diffusion-limited transport of the redox species from the electrolyte to the electrode interface. The appropriateness of the proposed fitting circuit model was evidenced by the small values of χ^2 on the order of 10^{-4}. The various electrodes were characterized via the Nyquist plots (Fig. 3), and the corresponding insets display the equivalent circuits. The R_{et} of bare ITO glass was 81.70 Ω cm^2, whereas APTES/ITO glass showed a much lower R_{et} of 23.39 Ω cm^2. Moreover, these results also indicated that APTES and the AuNPs were successfully modified on the surface of ITO and that the resulting composite-modified electrode showed higher conductivity than bare ITO, AuNPs/ITP and APTES/AuNPs/GCE. The decrease suggested the easy electron transfer at the electrode surface interface. Due to the protonation (NH_3^+) of the APTES amino groups in aqueous solution, the anionic probe $[Fe(CN)_6]^{3-/4-}$ had strong affinity to the polycationic layer, leading to an increase in its concentration at the solution-electrode interface. Therefore, the R_{et} was decreased, and meanwhile, the Y_0 (4.75 μF/cm) was relatively high. After the Au(MPA)-NPs were covalently attached onto the silane

layer, a decrease in Y_0 to 3.11 µF/cm^2 and an obvious increase in R_{et} to 109.3 Ωcm^2 were observed. This was because, for pH 7.4, the negatively charged Au(MPA)-NP carboxyl groups electrostatically repulsed the anionic probe at the solution-electrode interface. An APTES/ITO glass electrode modified by non-carboxyl-functionalized AuNPs in the absence of MPA capping was used in an EIS experiment to provide additional evidence that the carboxyl groups were present on the surface of the modified electrode. Non-Faradaic impedance biosensors show impedance in the absence of any redox probe. Bacteria detection is based on the impedance change upon the attachment of bacterial cells on an interdigitated microelectrode in the absence of any redox probe in the sample solution [45]. The semicircle diameter decreased, as shown in the corresponding Nyquist plot. This reduction corresponded to an obvious R_{et} decrease to 8.74 Ω cm^2, and it can be seen that charge transfer from the probe to the surface of the electrode was facile. Compared to the AuNP-modified electrode, the Au(MPA)-NP-modified electrode showed a much higher relative signal change, strongly confirming that the free carboxyl groups were abundant on the Au/(MPA)/APTES/ITO glass electrode surface. In addition, after the cardiac myoglobin protein antibody was covalently immobilized over the surface of the Au(MPA)-NPs and the nonspecific binding sites were subsequently blocked by BSA, a sharp increase in R_{et} to 187.8 Ω cm^2 along with a Y_0 decrease to 2.34 µF/cm^2 were observed. This indicated that the protein molecule was insulating, inhibiting mass and electron transfer from the probe to the electrode surface.
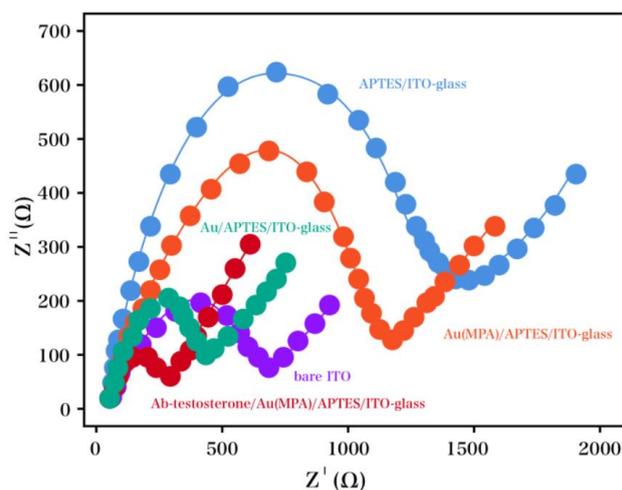

Figure 3. Nyquist plots at the bare ITO glass plate, APTES/ITO glass, Au(MPA)/APTES/ITO glass, Au/APTES/ITO glass and Ab-testosterone/Au(MPA)/APTES/ITO glass in pH 7.4 PBS (0.1 M KCl) + 2 mM [Fe(CN)$_6$]$^{3-}$/$^{4-}$.

A complex of antigen and antibody was formed due to the specific immunoreaction between Ab-testosterone and Ag-testosterone (its complementary target) on the electrode surface. A kinetic barrier was formed after an immunocomplex was generated, perturbing interfacial charge transfer at the bioelectrode/solution interface. Unlike under neutral conditions, in high pH buffer, the negative surface charge and the steric hindrance of testosterone increased with an increasing IFN-γ concentration. These effects gave rise to the redox reaction; therefore, the R_{ct} value increased [46]. The

increasing hindrance of the Faradaic reaction of the redox couple led to an increase in the charge transfer resistance and a corresponding decrease in the capacitance.
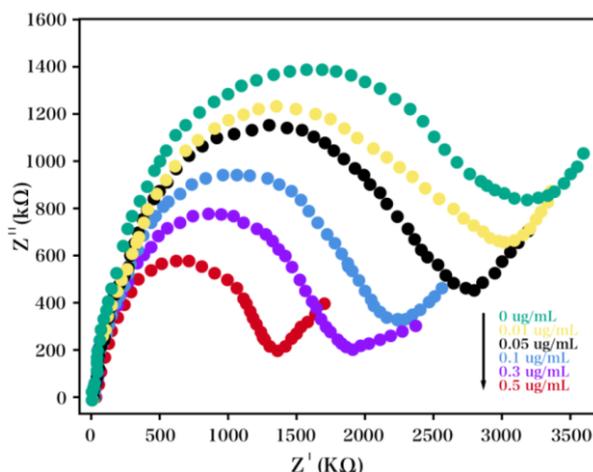

Figure 4. Faradaic impedance spectra (FIs) of the Ab-testosterone(BSA)/Au(MPA)/APTES/ITO-glass electrode before and after incubation with varying concentrations of Ag-testosterone in pH 7.4 PBS with 0.1 M KCl solution + 2 mM $[Fe(CN)_6]^{3-/4-}$.

The control sample was the sample solution in the absence of Ag-testosterone and target protein, with the sample response recorded as the R_{et}. Nyquist plots recorded after successive addition of aliquots of the target protein antigen at varying concentrations are shown in Fig. 4. Due to the interaction between the antibody and antigen, the added Ag-testosterone concentration was increased, and the diameter of the Nyquist circles was significantly increased, as shown in the plot. The Y_0 value was slightly decreased, suggesting that the capacitive performance of the bioelectrode decreased with immunoreaction.

Table 1. Content and recovery results using the Ab-testosterone/Au(MPA)/APTES/ITO glass electrode toward the detection of serum CK (n=3).

No.	Added (μg/mL)	Found (μg/mL)	Chromatographic detection (μg/mL)	Recovery (%)	RSD (%)
Saliva 1	0.05	0.0477	0.0521	95.40	4.02
Saliva 2	0.10	0.1051	0.1033	105.1	2.27

Table 2. Behavior comparison in testosterone detection using the Ab-testosterone/Au(MPA)/APTES/ITO glass electrode and methods proposed in other works.

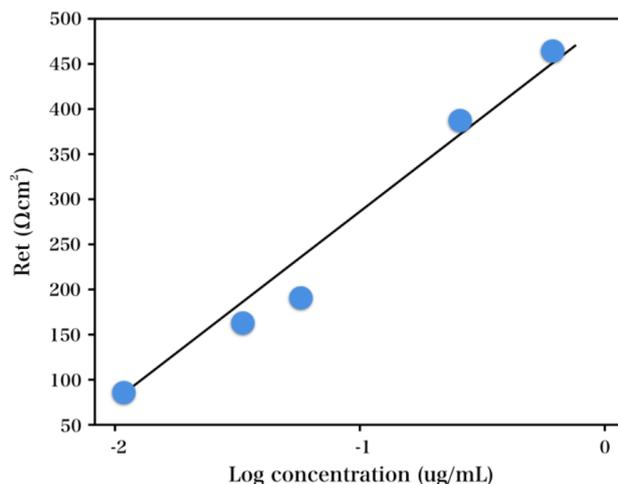| Detection method	LR (μg/mL)	DL (μg/mL)	Reference
Functionalized magnetic beads	0.0005-0.05	0.000017	[34]
Biomolecules/gold nanowires-doped sol–gel film	0.00012-0.0835	0.00001	[33]
AuNPs–CNT composite immunosensor	0.0001-0.01	0.000085	[47]
Ab-testosterone/Au(MPA)/APTES/ITO-glass	0.01-0.5	0.0039	This work

Figure 5. Calibration curve of the logarithm of testosterone concentration against the Ret collected from Ab-testosterone/Au(MPA)/APTES/ITO glass.

As deduced from Fig. 4, the variation of the specific electron charge transfer resistance ($\Delta R_{et} = (R_{et})_{after\ immunoreaction} - (R_{et})_{control}$) with the logarithmic value of the Ag-testosterone concentration (10 ng/mL to 0.5 µg/mL) was plotted (Fig. 5) to investigate the sensitivity of the proposed bioelectrode, displaying a LOD of 3.9 ng/mL (S/N=3). Furthermore, testosterone in saliva samples was analyzed using our developed electrode. Table 1 displays the results for the testosterone content in the above saliva specimens. Our proposed Ab-testosterone/Au(MPA)/APTES/ITO glass electrode could successfully determine testosterone in real specimens. In addition, Table 2 showed the performance comparison for testosterone detection between our proposed electrode and those reported in the literature.

4. CONCLUSIONS

This work presented the synthesis of AuNPs based on a proposed biosynthesis route, where the reduction agent was *Pithophora oedogonia.* An EIS biosensor that could rapidly diagnose polycystic ovarian syndrome was used for the measurement of testosterone concentrations. This developed sensor provided a linear concentration determination of testosterone (10 ng/mL to 0.5 µg/mL), with a LOD of 3.9 ng/mL.

References

1. U. Sinha, K. Sinharay, S. Saha, T.A. Longkumer, S.N. Baul and S.K. Pal, *Indian journal of endocrinology and metabolism*, 17 (2013) 304.
2. A. Makker, M.M. Goel, V. Das and A. Agarwal, *Gynecological Endocrinology*, 28 (2012) 175.

3. R.S. Legro, R.G. Brzyski, M.P. Diamond, C. Coutifaris, W.D. Schlaff, P. Casson, G.M. Christman, H. Huang, Q. Yan and R. Alvero, *New England Journal of Medicine*, 371 (2014) 119.
4. L. Skrgatic, D.P. Baldani, J. Cerne, P. Ferk and K. Gersak, *The Journal of steroid biochemistry and molecular biology*, 128 (2012) 107.
5. A.O. Lungu, E. Safar Zadeh, A. Goodling, E. Cochran and P. Gorden, *The journal of clinical endocrinology & Metabolism*, 97 (2012) 563.
6. B. Joshi, S. Mukherjee, A. Patil, A. Purandare, S. Chauhan and R. Vaidya, *Indian journal of endocrinology and metabolism*, 18 (2014) 317.
7. K.A. Walters, C.M. Allan and D.J. Handelsman, *Biology of reproduction*, 86 (2012) 149.
8. L. Pal, A. Berry, L. Coraluzzi, E. Kustan, C. Danton, J. Shaw and H. Taylor, *Gynecological Endocrinology*, 28 (2012) 965.
9. T. Tang, J.M. Lord, R.J. Norman, E. Yasmin and A.H. Balen, *The Cochrane Library*, (2012)
10. D. Dewailly, M.E. Lujan, E. Carmina, M.I. Cedars, J. Laven, R.J. Norman and H.F. Escobar-Morreale, *Human reproduction update*, 20 (2013) 334.
11. J. Münzker, D. Hofer, C. Trummer, M. Ulbing, A. Harger, T. Pieber, L. Owen, B. Keevil, G. Brabant and E. Lerchbaum, *The Journal of Clinical Endocrinology & Metabolism*, 100 (2015) 653.
12. L. Haqq, J. McFarlane, G. Dieberg and N. Smart, *Endocrine connections*, 3 (2014) 36.
13. E. Deligeoroglou, N. Vrachnis, N. Athanasopoulos, Z. Iliodromiti, S. Sifakis, S. Iliodromiti, C. Siristatidis and G. Creatsas, *Gynecological Endocrinology*, 28 (2012) 974.
14. K.F. Nicandri and K. Hoeger, *Current Opinion in Endocrinology, Diabetes and Obesity*, 19 (2012) 497.
15. N.K. Stepto, S. Cassar, A.E. Joham, S.K. Hutchison, C.L. Harrison, R.F. Goldstein and H.J. Teede, *Human reproduction*, 28 (2013) 777.
16. R. Tal, D.B. Seifer, M. Khanimov, H.E. Malter, R.V. Grazi and B. Leader, *American journal of obstetrics and gynecology*, 211 (2014) 59.
17. S. Iliodromiti, T.W. Kelsey, R.A. Anderson and S.M. Nelson, *The Journal of Clinical Endocrinology & Metabolism*, 98 (2013) 3332.
18. M. Maliqueo, H.E. Lara, F. Sánchez, B. Echiburú, N. Crisosto and T. Sir-Petermann, *European Journal of Obstetrics & Gynecology and Reproductive Biology*, 166 (2013) 151.
19. R. Li, Q. Zhang, D. Yang, S. Li, S. Lu, X. Wu, Z. Wei, X. Song, X. Wang and S. Fu, *Human reproduction*, 28 (2013) 2562.
20. P. Saxena, A. Prakash, A. Nigam and A. Mishra, *Indian journal of endocrinology and metabolism*, 16 (2012) 996.
21. E. Lerchbaum, V. Schwetz, A. Giuliani, T.R. Pieber and B. Obermayer-Pietsch, *Fertility and sterility*, 98 (2012) 1318.
22. I.A. Elgafor, *Archives of gynecology and obstetrics*, 288 (2013) 119.
23. H.Y. Zhang, C.X. Guo, F.F. Zhu, P.P. Qu, W.J. Lin and J. Xiong, *Archives of gynecology and obstetrics*, 287 (2013) 525.
24. L.J. Moran, H. Ko, M. Misso, K. Marsh, M. Noakes, M. Talbot, M. Frearson, M. Thondan, N. Stepto and H.J. Teede, *Journal of the Academy of Nutrition and Dietetics*, 113 (2013) 520.
25. N. Forouhi, S. Shab-Bidar and K. Djafarian, *Journal of Nutritional Sciences and Dietetics*, 1 (2015) 165.
26. Y. Suvarna, N. Maity, P. Kalra and M.C. Shivamurthy, *Journal of the Turkish German Gynecological Association*, 17 (2016) 6.
27. T. Van der Hoeven, *Biochemical and biophysical research communications*, 100 (1981) 1285.
28. C.H.L. Shackleton, H. Chuang, J. Kim, X. de la Torre and J. Segura, *Steroids*, 62 (1997) 523.
29. T.A. Ternes, H. Andersen, D. Gilberg and M. Bonerz, *Analytical Chemistry*, 74 (2002) 3498.
30. D.H. Catlin, D.A. Cowan, R. De la Torre, M. Donike, D. Fraisse, H. Oftebro, C.K. Hatton, B. Starcevic, M. Becchi and X. De La Torre, *Journal of mass spectrometry*, 31 (1996) 397.
31. R.J. Singh, *Steroids*, 73 (2008) 1339.

32. F. Matsui, E. Koh, K. Yamamoto, K. Sugimoto, H.-S. Sin, Y. Maeda, S. Honma and M. Namiki, *Endocrine journal*, 56 (2009) 1083.
33. K.-Z. Liang, J.-S. Qi, W.-J. Mu and Z.-G. Chen, *Journal of biochemical and biophysical methods*, 70 (2008) 1156.
34. M. Eguílaz, M. Moreno-Guzmán, S. Campuzano, A. González-Cortés, P. Yáñez-Sedeño and J.M. Pingarrón, *Biosensors and Bioelectronics*, 26 (2010) 517.
35. K. Inoue, P. Ferrante, Y. Hirano, T. Yasukawa, H. Shiku and T. Matsue, *Talanta*, 73 (2007) 886.
36. H. Lu, M.P. Kreuzer, K. Takkinen and G.G. Guilbault, *Biosensors and Bioelectronics*, 22 (2007) 1756.
37. R.N. Goyal, V.K. Gupta and S. Chatterjee, *Analytica chimica acta*, 657 (2010) 147.
38. V. Serafin, M. Eguílaz, L. Agüí, P. Yáñez-Sedeño and J.M. Pingarrón, *Electroanalysis*, 23 (2011) 169.
39. O. Laczka, F.J. del Campo, F.X. Muñoz-Pascual and E. Baldrich, *Analytical chemistry*, 83 (2011) 4037.
40. G. Li, M. Zhu, L. Ma, J. Yan, X. Lu, Y. Shen and Y. Wan, *ACS applied materials & interfaces*, 8 (2016) 13830.
41. V. Vilas, D. Philip and J. Mathew, *Journal of Molecular Liquids*, 221 (2016) 179.
42. S. Pakapongpan, R. Palangsuntikul and W. Surareungchai, *Electrochimica Acta*, 56 (2011) 6831.
43. Y.-H. Lin and P.-Y. Peng, *Anal. Chim. Acta.*, 869 (2015) 34.
44. M. Li, S. Biswas, M.H. Nantz, R.M. Higashi, X.A. Fu and A. Chem, *Analytical Chemistry*, 84 (2012) 1288.
45. S.M. Radke and E.C. Alocilja, *Biosensors & bioelectronics*, 20 (2005) 1662.
46. M. Reynard, D. Turner and C. Navarrete, *International Journal of Immunogenetics*, 27 (2000) 241.
47. V. Serafin, M. Eguílaz, L. Agüí, P. Yáñez-Sedeño and J. Pingarrón, *Electroanalysis*, 23 (2011) 169